

Chapter 11

Copper-Labeled Radiopharmaceuticals in Oncology

Hiroaki Kurihara

Abstract Among copper (Cu) isotopes, radioactive ^{60}Cu , ^{61}Cu , ^{62}Cu , ^{64}Cu , and ^{67}Cu have potential to be used in biomedical research. ^{60}Cu , ^{61}Cu , and ^{62}Cu can be used in positron emission tomography (PET) diagnostic imaging. Similarly, ^{67}Cu can be used in gamma imaging, and it is potentially suitable for diagnostic PET imaging and radiotherapy. These five radioactive Cu isotopes can be produced in a cyclotron. ^{62}Cu and ^{64}Cu are the most frequently used Cu radioisotopes because of their availability. Recently, interest in Cu radiopharmaceuticals has been increasing because they have been conjugated to antibody proteins, peptides, nanoparticles, and small molecular compounds for preclinical and clinical studies. This chapter provides an overview of the preparation, chemical, and clinical applications of Cu-labeled radiopharmaceuticals.

11.1 Introduction

Copper (Cu) is a transition metal with the atomic number 29, which is an important and widespread element in the world. It has been known since ancient times, and it is used as currency in many countries. Cu has 2 stable isotopes, ^{63}Cu and ^{65}Cu , and 27 unstable radioisotopes with decades of research. Most radioactive Cu isotopes have half-lives of less than 1 min; however, ^{60}Cu , ^{61}Cu , ^{62}Cu , ^{64}Cu , and ^{67}Cu have relatively longer half-lives ranging from 10 min to 62 h, and they are suitable for potential use in biomedical research. For example, ^{64}Cu was used to evaluate Cu metabolism and to assess patients with Wilson disease in 1982 [1]. In the last few decades, the development of imaging modalities and radiolabeling techniques has permitted to overcome the limits in anatomical imaging, allowing for a shift toward molecular imaging. By not only generating high-resolution images of the human body but also assessing the distribution of specific molecules noninvasively, molecular imaging helps physicians to diagnose illness and choose appropriate treatment regimens [2]. This new approach with radioactive Cu offers further opportunities for

H. Kurihara (✉)
National Cancer Center, Tokyo, Japan
e-mail: hikuriha@ncc.go.jp

Table 11.1 Decay characteristic and production property of copper radiopharmaceutical

Isotope	Nuclear production reaction	Half-life	β^+ MeV (%)	β^- MeV (%)	EC (%)	γ MeV (%)
^{60}Cu	$^{60}\text{Ni}(p,n)^{60}\text{Cu}$	23.4 min	3.92 (6%)	–	7.4%	0.85 (15%)
	$^{59}\text{Co}(^3\text{He},2n)^{60}\text{Cu}$		3.00 (18%)			1.33 (80%)
			2.00 (69%)			1.76 (52%)
						2.13 (6%)
^{61}Cu	$^{61}\text{Ni}(p,n)^{61}\text{Cu}$	3.3 h	1.22 (60%)	–	40%	0.284 (12%)
	$^{59}\text{Co}(^3\text{He},n)^{60}\text{Cu}$					0.38 (3%)
						0.511 (120%)
^{62}Cu	$^{62}\text{Ni}(p,n)^{62}\text{Cu}$	9.7 min	2.91 (98%)	–	2%	0.511 (194%)
	$^{60}\text{Cu}(p,2n)^{62}\text{Zn}$: $^{62}\text{Zn}/^{62}\text{Cu}$					
^{64}Cu	$^{64}\text{Ni}(p,n)^{64}\text{Cu}$	12.7 h	0.655 (19.3%)	0.573 (39.6%)	41%	1.35 (0.6%)
						0.511 (38.6%)
^{67}Cu	$^{68}\text{Zn}(p,2p)^{67}\text{Cu}$	62.0 h	–	0.577 (20%)	–	0.184 (40%)
	$^{67}\text{Zn}(n,p)^{67}\text{Cu}$			0.484 (35%)		0.092 (23%)
				0.395 (45%)		

clinical research, diagnostic imaging, and targeted radiotherapy. Copper isotopes with atomic masses below 63 tend to undergo β^+ decay and can be used in PET diagnostic imaging. In contrast, isotopes with atomic masses above 65 tend to undergo β^- decay and can be used in gamma imaging and radiotherapy. Moreover, radioactive ^{64}Cu undergoes both β^+ and β^- decay, so ^{64}Cu may be suitable for use in diagnostic PET imaging, gamma imaging, and radiotherapy (Table 11.1).

Availability is an important consideration for the widespread use of any radioisotope in medicine. In this regard, the half-lives of ^{60}Cu and ^{61}Cu seem to be too short for commercial delivery of routine clinical isotopes in nuclear medicine practice. ^{62}Cu also has a short half-life, 10 min, but it can be easily produced on-site using a $^{62}\text{Zn}/^{62}\text{Cu}$ generator and readily available for clinical studies. For example, $^{62}\text{Cu}(\text{II})$ -diacetyl-bis(N^4 -methylthiosemicarbazone) (^{62}Cu -ATSM), an imaging agent targeting hypoxia, can be prepared for clinical research using a simple procedure with generator-produced ^{62}Cu [3]. ^{64}Cu has also been available for clinical research because it can be produced in a baby cyclotron located in a hospital. It has a relatively longer half-life (12.7 h), which makes it possible to prepare ^{64}Cu -labeled radiopharmaceuticals. Despite the fact that ^{64}Cu has a low positron branching ratio (17.6%), some researchers cite ^{64}Cu -labeled radiopharmaceuticals, which can be used as PET probes that provide better intrinsic image resolution with low β^+ maximal energy [4, 5]. ^{67}Cu undergoes β^- decay and is potentially useful for targeted radiotherapy, but due to limited availability, few researchers have reported its use thus far [6, 7].

In keeping with this notion, Cu-labeled radiopharmaceuticals may have clinical impact in oncology. In this chapter, an overview of the production and properties of

radioactive Cu, the chemistry of Cu radiopharmaceuticals, and clinical applications for Cu radiopharmaceuticals is provided.

11.2 Production and Properties of Radioactive Cu

With advances in the medical sciences, Cu has gained a lot of attention, especially in molecular imaging. Several radioactive Cu isotopes can be obtained by bombarding nickel (Ni), cobalt (Co), or Zn with proton (p), neutron (n), or helium (He) in a cyclotron or reactor, but proper selection of the radionuclide to generate radiopharmaceuticals is critical. It depends upon several factors: half-life, radionuclide energy, cost, and availability. The half-life of the radionuclide should allow for sufficient uptake and distribution to yield high image quality. The energy of the radionuclide emission should be appropriate for proper detection by the equipment [8]. This section provides an overview of the production and properties of five radioactive Cu isotopes because they have the most potential for molecular imaging applications (^{60}Cu , ^{61}Cu , ^{62}Cu , and ^{64}Cu) and in vivo targeted radiotherapy (^{64}Cu and ^{67}Cu) [8].

11.2.1 ^{60}Cu

^{60}Cu can be produced in a medical cyclotron at a relatively low cost, using proton or deuteron bombardment of enriched ^{60}Ni targets [9, 10]. Other methods of production, such as the $^{59}\text{Co}(^3\text{He},2n)^{60}\text{Cu}$ reaction, have been reported [11, 12]. ^{60}Cu is a proton-rich nuclide with a half-life of 23.7 min to its stable ^{60}Ni isotopes, through a combination of positron decay and electron capture processes. Thus, ^{60}Cu is a potential candidate tracer for PET imaging. However, its relatively high-energy positron (maximum energy, 3.92 MeV) and numerous gamma concurrent emissions in cascades (most notably 0.85 MeV, 15%; 1.33 MeV, 80%; 1.76 MeV, 52%; and 2.13 MeV, 6%) affect image quality. These additional γ -photons can downscatter into the acceptance energy window of the scanner and supply incorrect positional information, which results in higher background activity and poorer image quality and accuracy.

11.2.2 ^{61}Cu

^{61}Cu can be produced by proton bombardment of ^{61}Ni targets or ^3He bombardment of ^{59}Co targets, using a medical cyclotron. The half-life of ^{61}Cu (3.3 h) is longer than that of ^{60}Cu and ^{62}Cu , which makes ^{61}Cu a better choice for prolonged imaging with slower kinetics. However, this isotope is not currently popular because it requires

highly enriched Ni targets or high-energy ^3H beams, which limits the accessibility of ^{61}Cu [8, 12–15]. More economical production methods should be developed before clinical use [16, 17].

11.2.3 ^{62}Cu

^{62}Cu is a proton-rich nuclide that decays with a half-life of 9.7 min to its stable ^{62}Ni isotope, through a combination of positron decay (98%) and electron capture processes (2%). It can be produced using a $^{62}\text{Zn}/^{62}\text{Cu}$ generator system. Current $^{62}\text{Zn}/^{62}\text{Cu}$ generators achieve high elution efficiency, approximately 96%, using a small volume (approximately 3 ml) of eluate, with very low breakthrough of ^{62}Zn [18]. One disadvantage of $^{62}\text{Zn}/^{62}\text{Cu}$ generators is that they can be used for only 1–2 days because of the relatively short half-life of parent ^{62}Zn (half-life, 9.2 h). However, this method has been proven to be highly useful as a source of ^{62}Cu for the synthesis of ^{62}Cu -labeled compounds [18, 19]. ^{62}Cu can also be produced with a medical cyclotron, using proton- or deuteron-induced reactions on enriched ^{62}Ni targets. However, this cyclotron method is not popular in nuclear medicine because its short half-life limits the final yield of ^{62}Cu -labeled radiopharmaceuticals prepared from the irradiated target [9]. ^{62}Cu from a $^{62}\text{Zn}/^{62}\text{Cu}$ generator is currently the most intensively studied Cu radioisotope after ^{64}Cu [8, 18, 19].

11.2.4 ^{64}Cu

^{64}Cu decays via three processes: positron decay, electron capture, and beta decay. This property allows ^{64}Cu isotopes to be used for both PET imaging and radiotherapy. With a half-life of 12.7 h, ^{64}Cu is ideally suited for PET studies that require a longer-lived nuclide. Distribution of ^{64}Cu radiopharmaceuticals from the production site to other facilities is possible, and PET imaging can be conducted up to 48 h after tracer administration. Moreover, because ^{64}Cu has a maximum positron energy of 0.655 MeV, similar to that of ^{18}F , the resulting PET images are of high quality and are the best obtainable with any of the positron-emitting radioactive Cu isotope. Since 39.6% of ^{64}Cu decay occurs by β^- emission, there is a possibility of therapeutic applications with this nuclide.

^{64}Cu can be produced using either a cyclotron or a reactor. Currently, the most common ^{64}Cu production method utilizes the $^{64}\text{Ni}(p,n)^{64}\text{Cu}$ reaction, which can be conducted even with a medical cyclotron [20, 21]. The target for producing ^{64}Cu is enriched ^{64}Ni as follows: a ^{64}Ni target is electroplated on a gold disk at a thickness of 50–100 μm and electroplating is performed at 2.5 V, at currents ranging from 5 to 15 mA, which is completed in 12–24 h. The ^{64}Ni target is then bombarded with a $50 \pm 3 \mu\text{A}$ proton current and after bombardment, ^{64}Cu can be purified from the ^{64}Ni target and other contaminants using an anion exchange column. Target ^{64}Ni can be recovered and reused [22] with this method, and sufficient quantities of purified

^{64}Cu for diagnostic imaging and therapeutic application can be obtained. The radio-nuclide purity of the ^{64}Cu generated using this process is over 99%. The specific activity of ^{64}Cu may range widely because ubiquitous cold Cu may contaminate the procedure. Producing high levels of ^{64}Cu -specific activity requires careful management to maintain a metal-free environment for ^{64}Cu preparation.

Another method of ^{64}Cu production using the $^{64}\text{Zn}(n,p)^{64}\text{Cu}$ reaction in a nuclear reactor has been described elsewhere [23, 24]. However, this reaction has waste concerns and undesirable byproducts such as ^{65}Zn (half-life, 245 d), which limits the practicality of this production method.

11.2.5 ^{67}Cu

^{67}Cu is the longest living Cu radioisotope. It undergoes β^- decay with a half-life of 62 h. The growing interest in targeted radiotherapy has increased the demand for this β^- emitting isotope. ^{67}Cu can be produced via several reactions with Zn, but it is one of the most difficult radioactive Cu isotopes to produce. A $^{68}\text{Zn}(p,2p)^{67}\text{Cu}$ nuclear reaction, the most popular reaction for ^{67}Cu production, requires a high-energy proton beam (20–70 MeV) [25]. The other method to produce ^{67}Cu is via the $^{67}\text{Zn}(n,p)^{67}\text{Cu}$ reaction. Although this appears to be simple, it requires a fast neutron flux reactor, and the use of this reactor reaction for extended productions and medical applications is associated with waste concerns and undesirable side reactions. Recently, a novel larger-scale production method for ^{67}Cu using a high-energy proton accelerator has been described, which may allow for commercial delivery of ^{67}Cu to become available in the near future [26].

11.3 Chemistry of Cu Radiopharmaceuticals

Radioactive Cu offers the ability to exploit unique aspects of Cu radiopharmaceutical chemistry. In aqueous solution, Cu is mainly restricted to oxidation states I and II. Cu(I) generally exists only in aqueous solution as a strong complex, since the free ion is disproportionate to Cu^{2+} and Cu^0 metal. A Cu^{3+} ion may exist under certain conditions, but it is not stable in the biochemical environment because of its strong oxidizing properties. On the other hand, Cu(II) prefers a coordination number of 4. In general, it can be chelated by ligands arranged in a square planar configuration.

So far, many ligands that can chelate Cu(II), such as thiosemicarbazones and macrocyclic bifunctional chelators, have been previously reported. Cu(II)-thiosemicarbazones were first designed in 1964 as anticancer agents and evaluated as radiopharmaceuticals since 1987 [27]. Thiosemicarbazones labeled with radioactive Cu have been developed to image blood flow and hypoxia. Other bifunctional chelators are known to be suitable for conjugating radioactive Cu to antibody proteins or peptides. In order for these radioactive Cu isotopes chelated with biomolecules to be effective, high thermodynamic and in vivo stability of the radiolabeled

biomolecules are required. For example, complexes of Cu(II) and bifunctional chelators such as ethylenediaminetetraacetic acid (EDTA) and diethylenetriaminepentaacetic acid (DTPA) were not stable enough *in vivo* because they rapidly dissociate in human serum and Cu(II) binds to human serum albumin [28]. Other macrocyclic chelators have varying degrees of biological stability. For instance, Cu-labeled 1,4,7,10-tetraazacyclododecane-1,4,7,10-tetraacetic acid (DOTA) is more stable in serum than Cu-labeled 1,4,8,11-tetraazacyclotetradecane-*N,N',N'',N'''*-tetraacetic acid (TETA) compounds [29]. In addition, the charge of the Cu(II) complex has an important effect on biodistribution. Negatively charged complexes are excreted from the body more rapidly than positively charged ones [30] Fig. 11.1.

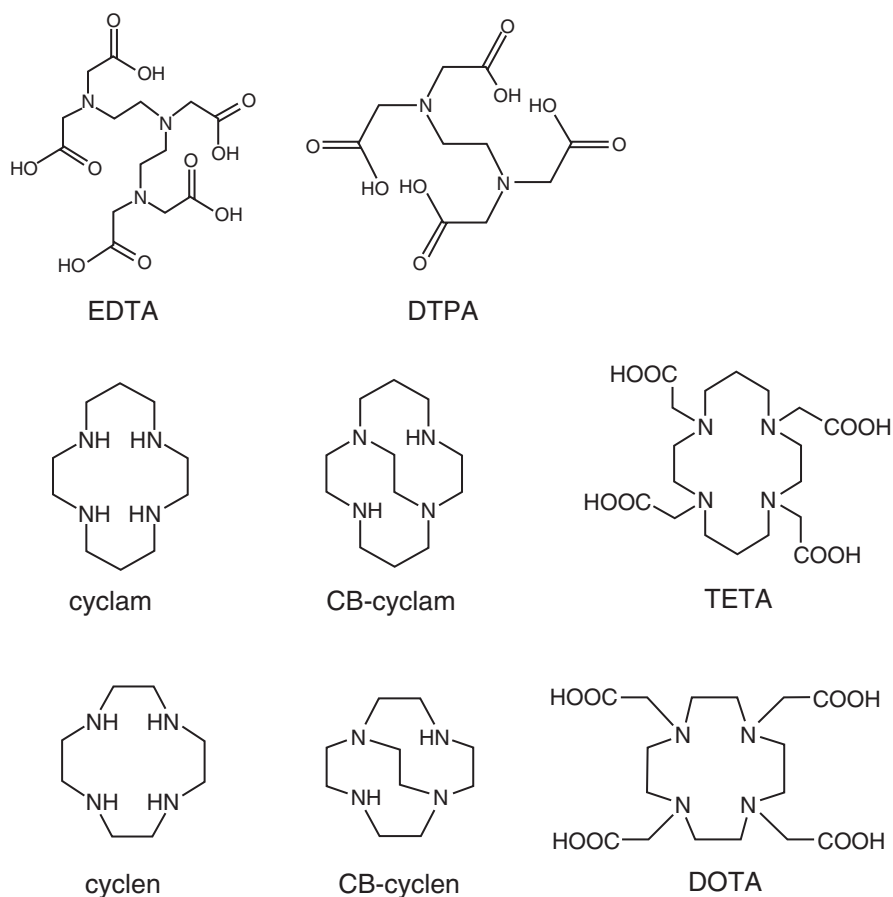


Fig. 11.1 Chemical structures of several bifunctional chelators. *EDTA* ethylenediaminetetraacetic acid, *DTPA* diethylene triamine pentaacetic acid, *cyclam* 1,4,8,11-tetraazacyclotetradecane, *cyclen* 1,4,7,10-tetraazacyclododecane, *TETA* 1,4,8,11-tetraazacyclotetradecane-*N,N',N'',N'''*-tetraacetic acid, *DOTA* 1,4,7,10-tetraazacyclododecane-1,4,7,10-tetraacetic acid, *CB-cyclam* cross-bridged cyclam, *CB-cyclen* cross-bridged cyclen

11.4 Clinical Applications of Radioactive Cu

11.4.1 *Cu-Labeled Agents to Assess Blood Flow*

The design of radiopharmaceutical agents for diagnostic imaging is dependent on the desired characteristics of the molecular targets. Due to the high rates of morbidity and mortality associated with cardiovascular and cerebrovascular diseases, myocardial and cerebral perfusion tests are important clinical applications. To date, there are single photon emission computed tomography (SPECT) agents that routinely use current clinical nuclear medicine procedures. However, PET has the potential to improve diagnostic accuracy in these applications, which has led to an interest in developing radioactive Cu-labeled blood flow agents for myocardial and cerebral perfusion imaging. Blood flow agents have been evaluated as ligands that form lipophilic uncharged complexes with Cu. These Cu complexes have been designed to be sufficiently stable to clear the blood and diffuse into tissues of interest, such as the brain, heart, kidneys, and even tumors. Cu complexes that release the Cu radionuclide after reaching the tissue of interest are advantageous, because the radioactive Cu can then be trapped in the tissue of interest without the need to washout.

Cu-bis(thiosemicarbazone) (Cu-BTS) complexes have been extensively evaluated for their use as Cu radiopharmaceuticals in PET perfusion imaging. Pyruvaldehyde bis(*N*⁴-methylthiosemicarbazone)Cu (Cu-PTSM) is the first clinically used and widely studied Cu-BTS complex. Human PET studies with ⁶²Cu-PTSM have demonstrated that the tracer provides high-quality PET images of the heart, in which regional myocardial perfusion is accurately delineated [31]. In addition, ⁶²Cu-PTSM is a sufficiently sensitive tracer for regional cerebral blood flow. It has been used to detect regional cerebral perfusion impairment in patients who suffered a stroke [32]. However, ⁶²Cu-PTSM binds to human serum albumin reversibly, which impairs its ability to quantify myocardial perfusion under hyperemic conditions. To overcome this problem, next-generation Cu-BTS complexes that may be suitable for quantification of myocardial perfusion with PET have been developed.

11.4.2 *Cu-Labeled Hypoxia Imaging Agents*

Hypoxic tissue in the brain, heart, and tumors is considered an important imaging target. In oncology, it frequently suggested that a hypoxia imaging technique may help select cancer patients, who would benefit from treatments that overcome, circumvent, or take advantage of the hypoxic environment. This is because tumor hypoxia is an important biological characteristic that leads to radioresistance during cancer treatment. Imaging could also be used to demonstrate the degree to which reoxygenation of tumors occurs during radiotherapy. Many challenges in hypoxia

imaging with magnetic resonance, optical, and nuclear imaging have been reported [33]. For instance, magnetic resonance imaging (MRI) methods are attractive because they avoid the use of radioactivity and MRI equipment is widely available, but hypoxia-reporter molecules for MRA require relatively large quantities of the reporter. PET has high sensitivity and spatial resolution, which has the advantage of visualizing molecular events in living human tissue, which makes it a leading tool for imaging hypoxia. Hypoxia-reporter molecules used in PET can be divided into two groups based on chemical structure: nitroimidazole compounds and non-imidazole imaging agents [34]. The nitroimidazole compounds include ^{18}F -Fluoromisonidazole (^{18}F -FMISO), ^{18}F -fluoroerythronitroimidazole (^{18}F -FETNIM), and ^{18}F -fluoroazomycin-arabinofuranoside (^{18}F -FAZA). Non-imidazole imaging agents contain a metal complex of radioactive Cu with diacetyl-bis(N^4 -methylthiosemicarbazone) (ATSM). The following section will focus on agents with radioactive Cu-ATSM, which are the leading contenders for human applications [35].

11.4.2.1 Radioactive Cu-ATSM

The proposed mechanisms of Cu(II)-ATSM accumulation in hypoxic cells include Cu(II)-ATSM, an uncharged lipophilic, highly membrane-permeable molecule, which can undergo reduction by cellular-reducing equivalents and be converted to $[\text{Cu}(\text{I})\text{-ATSM}]^-$. Then tetrahedral Cu(I) can be easily released from ATSM to form strong Cu(I) complexes or be converted to Cu^0 (Cu metal) or Cu^{2+} , which subsequently forms complexes with proteins and is trapped in hypoxic cells (Fig. 11.2).

Radioactive Cu-ATSM can be readily synthesized with a one-step simple reaction using radioactive Cu and the substrate ATSM [36]. In brief, 10 μl of ATSM dissolved in dimethyl sulfoxide solution (1 mg/ml) is added to hydrochloride-buffered radioactive Cu chloride for 2 min. Next, radioactive Cu-ATSM is eluted with ethanol using a C18 Sep-Pak cartridge. After approximately 80% of the ethanol has been evaporated with blown argon gas, the remaining radioactive Cu-ATSM is diluted in saline for injection. Quality analyses showed high radiochemical purity (>95%) and a high yield (>95%) of the final radioactive product [37, 38].

For PET imaging, there are four different positron-emitting Cu isotopes: ^{60}Cu (half-life, 0.39 h; β^+ , 93%), ^{61}Cu (half-life, 3.3 h; β^+ , 60%), ^{62}Cu (half-life, 0.16 h; β^+ , 98%), and ^{64}Cu (half-life, 12.7 h; β^+ , 19.3%). ^{60}Cu , ^{61}Cu , and ^{64}Cu can be produced in small cyclotrons, and ^{62}Cu can be obtained via a $^{62}\text{Zn}/^{62}\text{Cu}$ generator system.

Since Fujibayashi et al. have reported the use of ^{62}Cu -ATSM as a hypoxia imaging agent in 1997 [38], numerous studies have demonstrated that ^{60}Cu -ATSM uptake can predict tumor behavior and response to therapy in patients with non-small cell lung cancer [39], cervical cancer [40], colorectal carcinoma [41], and malignant glioma [3]. Chao et al. demonstrated the feasibility of using ^{60}Cu -ATSM imaging to identify hypoxic tumor sub-volume, through co-registration of computed tomography and ^{60}Cu -ATSM PET images in order to plan a patient's course of radiotherapy

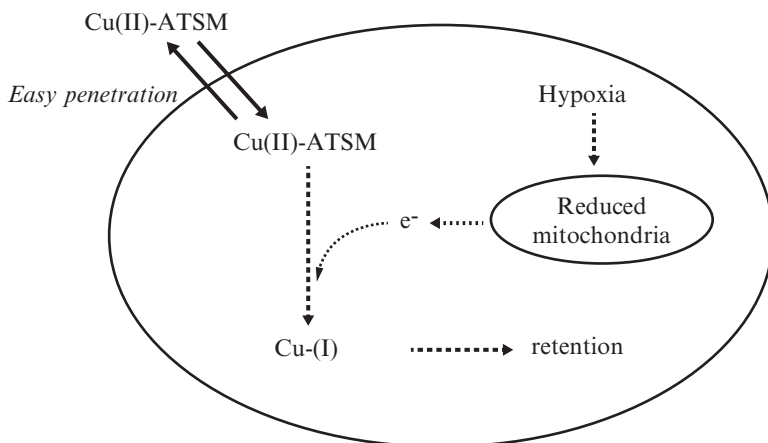


Fig. 11.2 Proposed retention mechanism of Cu-ATSM in a hypoxic cell. Cu(II)-ATSM is a neutral lipophilic molecule, which can easily penetrate cell membrane. In normoxic cells, the neutral lipophilic Cu(II)-ATSM can be easily washed out (*solid arrow*). In hypoxic cells, Cu(II)-ATSM can be converted with electron (e^-) supplied from abnormally reduced mitochondria to Cu(I), which is entrapped in the cells

and perform intensity-modulated radiation therapy [42]. When Lewis et al. compared image quality and tumor uptake of ^{60}Cu -ATSM and ^{64}Cu -ATSM in ten patients with cervical carcinoma, they concluded that both were safe radiopharmaceuticals and that image quality with ^{64}Cu -ATSM is better than that with ^{60}Cu -ATSM due to reduced background [43]. In a study by Dehdashti et al., ^{60}Cu -ATSM uptake (tumor-to-muscle ratio threshold of 3.5) in 38 patients with cervical cancer was inversely related to progression-free survival and cause-specific survival. Similarly, ^{62}Cu -ATSM PET can visualize lung adenocarcinoma and enlarged mediastinal lymph node [44]. Moreover, ^{62}Cu -ATSM PET can help identify highly malignant gliomas, while ^{62}Cu -ATSM T/B ratio may predict hypoxia-inducible factor-1 α (HIF-1 α) expression. This suggests that ^{62}Cu -ATSM is a suitable biomarker for predicting high-grade malignancy and tissue hypoxia in patients with glioma [45]. An example of a clinical ^{62}Cu -ATSM PET/CT study is shown in Fig. 11.3.

11.4.2.2 Clinical Role of Hypoxia Imaging in Oncology

Tumor hypoxia is commonly present in tumor tissues, where it poses a significant challenge to the curability of human tumors, which can lead to resistance to therapy and enhanced tumor progression. Imaging tumor hypoxia has two major clinical uses: (a) select patients, who may show a better response to curative treatments designed to overcome the limitations of hypoxia and (b) reveal by serial imaging that the treatment strategy reduce the extent of regional hypoxia. Hypoxia imaging may also allow for better identification of a subpopulation of cancer patients, who would benefit from novel targeted anti-hypoxia therapies.

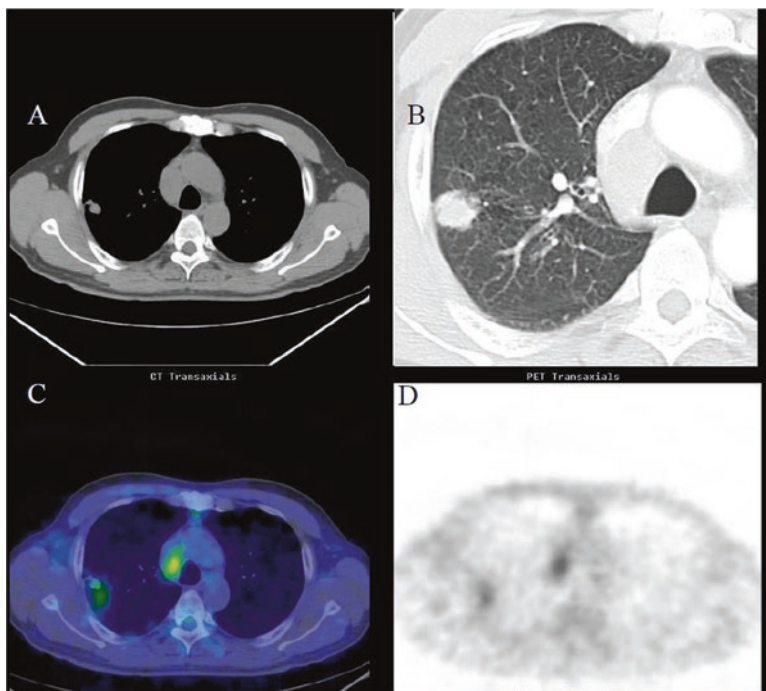


Fig. 11.3 A clinical case of the ^{62}Cu -ATSM PET/CT application (Courtesy of Hirofumi Fujii, M.D., National Cancer Center Hospital East). A 60-year-old man suffering from lung adenocarcinoma was examined with ^{62}Cu -ATSM PET/CT study. (a, b) CT images show lung tumor in right upper lobe and mediastinal lymphadenopathy. (c, d) ^{62}Cu -ATSM PET/CT fusion image and PET image revealed high accumulation in the lung tumor and the enlarged lymph node

11.4.3 *Cu-Labeled Antibodies*

Many novel molecular targets to treat cancer have been discovered, which has led to the development of molecularly targeted drugs. These drugs are cornerstones of precision medicine that use information from a patient genetic to diagnose, treat, and prevent the disease. Therapeutic monoclonal antibodies have played a major role in molecularly targeted therapy, and there are demands for the use of radiolabeled antibodies in molecular imaging, which can identify the presence of specific targets throughout the body, in a noninvasive approach.

For example, trastuzumab, a humanized monoclonal antibody against human epidermal growth factor receptor 2 (HER2), is a widely used therapeutic antibody. The application of trastuzumab-mediated technology is a well-established strategy to target HER2-positive breast cancer [46–50]. HER2 is overexpressed in 25–30% of patients with breast cancer and is directly involved in tumor cell survival, proliferation, maturation, metastasis, and angiogenesis [51, 52]. HER2 expression is routinely determined using immunohistochemistry (IHC) or fluorescence in situ

hybridization [53]. However, technical problems can arise when lesions cannot be easily accessed for core needle biopsy [54]. In addition, HER2 expression can vary during the course of the disease [55], even between tumors in the same patient [56]. To overcome these problems, a novel noninvasive technique such as HER2 PET imaging is desirable for conclusive assessment of HER2 expression.

So far, molecular PET imaging for HER2 has been studied intensively with trastuzumab labeled with ^{124}I , ^{86}Y , ^{76}Br , ^{89}Zr , or ^{64}Cu [4, 57]. For PET imaging, ^{64}Cu can be a useful radioactive Cu nuclear agent because of its relatively longer half-life. The following section will focus on anti-HER2 molecular imaging with ^{64}Cu -labeled trastuzumab in humans.

Briefly, the preparation of ^{64}Cu -labeled trastuzumab occurs as follows: after purification of the trastuzumab IgG (Herceptin®) by ultrafiltration with phosphate-buffered saline (PBS), the PBS-filtered trastuzumab is added to 1,4,7,10-tetraazacyclododecane-1,4,7,10-tetraacetic acid (DOTA) mono-*N*-hydroxysuccinimide ester and dissolved in water. After incubation at 40 °C for 3 h, crude DOTA-trastuzumab is purified with PBS by using a PD-10 column. The PBS buffer, including DOTA-trastuzumab, is exchanged for a sodium acetate buffer (100 mM, pH 6.5) by filtration. ^{64}Cu -DOTA-trastuzumab is then prepared by adding previously purified ^{64}Cu (see “Production of Radioactive Cu”) to the DOTA-trastuzumab acetate solution, followed by incubation for 1 h at 40 °C. Lastly, the reaction mixture is sterilized by filtration through a 0.22- μm filter [4]. In sum, radio-labeling achieves a specific activity of approximately 350 GBq/ μmol and a 98% radiochemical purity. Using the ^{64}Cu -trastuzumab PET imaging technique, primary tumor lesions larger than 2 cm in diameter and metastatic brain lesions larger than 1 cm in diameter can be visualized [4, 58]. Typical ^{64}Cu -DOTA-trastuzumab PET images in patients with HER2-positive breast cancer are shown in Fig. 11.4. Remarkably, HER2 specificity of ^{64}Cu -DOTA-trastuzumab has been confirmed in human samples, prepared from surgically removed tumor specimens by autoradiography, IHC, and liquid chromatography-tandem mass spectrometry (LC-MS/MS) [4, 58]. As an example, Fig. 11.5 shows an autoradiograph of a frozen section prepared from a tumor specimen, in which high signal accumulation can be observed in the area where HER2-positive cells were seen by IHC.

Another HER2 PET imaging with a ^{89}Zr -trastuzumab probe can successfully visualize HER2-positive tumors in humans. Due to the relatively longer half-life of Zr-89, ^{89}Zr -trastuzumab provides clearer images. However, it involves higher radiation exposure [59]. In contrast, the shorter half-life of ^{64}Cu involves lower radiation exposure but provides images with non-specific activity in the blood [4, 60]. Although improvements are still needed, these imaging techniques can be used to serially monitor HER2 tumor status, during HER2 targeted therapy and also serve to evaluate patients with tumors that are not easily accessible with core needle biopsies.

Recently, several novel HER2 inhibitors have been developed and approved, such as lapatinib, pertuzumab, and trastuzumab emtansine (T-DM1). Monitoring changes in HER2 expression at tumor sites may help physicians determine which HER2 inhibitor should be used during different phases of treatment or if non-HER2

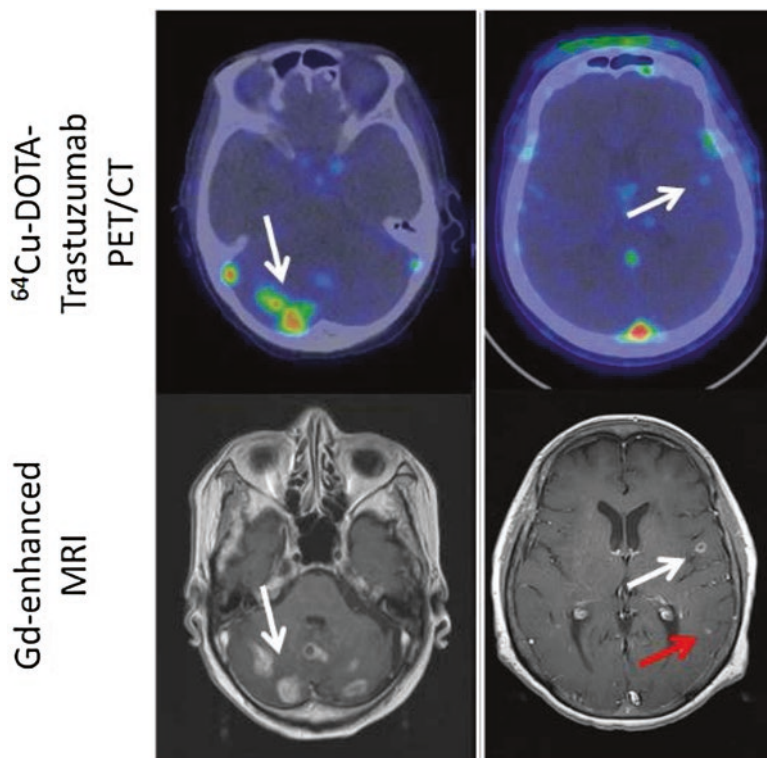


Fig. 11.4 ^{64}Cu -DOTA-trastuzumab PET images of metastatic brain tumors in patients with HER2-positive primary breast cancer. The *white arrows* show the metastatic brain tumors. *Upper panels*, ^{64}Cu -DOTA-trastuzumab PET images; *lower panels*, Gd-DTPA-enhanced T1-weighted MRI images. *White arrows* indicate metastatic brain lesions detectable by both MRI and ^{64}Cu -DOTA-trastuzumab PET, and *red arrow* indicates a lesion detectable by MRI but not by ^{64}Cu -DOTA-trastuzumab PET

inhibitors should be used instead. Preclinical results with HER2 imaging are promising, but clinical data are still limited. Clinical HER2 PET imaging findings may support the further development and exploration for the potential of this technique.

11.4.4 *Cu-Labeled Peptides*

Most current Cu radiopharmaceutical research focuses on ^{64}Cu -labeled peptides for targeted cancer therapy or imaging. They consist of a targeting peptide such as bombesin or an octreotide analogue, a linker, and a bifunctional chelator such as TETA or DOTA. The peptide binds to a specific receptor expressed by cancer cells, while the ^{64}Cu moiety allows for localization of the tumor by PET. For example,

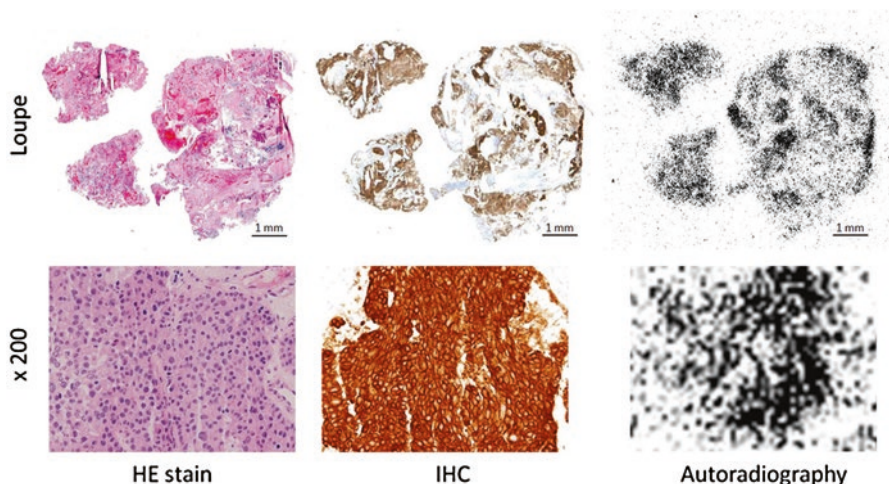


Fig. 11.5 Histological distribution of ^{64}Cu -radioactivity in HER2-positive tumors. *Left column*, HE staining; *middle column*, IHC; *right column*, autoradiography. Loupe images (*upper panels*) show identical distribution of radioactivity and location of HER2-positive tumor cells for HE stain, IHC, and autoradiography samples. Magnified images (*lower panels*, $\times 200$) confirmed the radioactivity and HER2-positive status of tumor cells

octreotide, a peptide of eight amino acids, is a somatostatin analogue that has affinity for somatostatin receptors. Targeting of somatostatin receptors in tumors has been a goal of cancer treatment and diagnosis. In the first-in-human study, ^{64}Cu -DOTATATE PET was found to be useful to image the somatostatin receptor [61]. Compared with ^{111}In -DTPA-octreotide SPECT, ^{64}Cu -DOTATATE PET provided superior image quality, detected more true-positive lesions, and was associated with a lower radiation burden.

11.5 Summary

Radioactive Cu isotopes are playing a larger role in both PET imaging and targeted radiotherapy. The versatility of Cu isotopes gives them a strong position in the development of new pharmaceuticals. With a $^{62}\text{Zn}/^{62}\text{Cu}$ generator system, ^{62}Cu can be obtained easily in hospital settings for use in PET imaging. ^{64}Cu can be used in hospitals, since its longer half-life allows for production at regional or national cyclotron facilities and distributed to local nuclear medicine departments. In addition, high doses of ^{64}Cu -labeled radiopharmaceuticals can be used for targeted radiotherapy. Radioactive Cu could be suitable for theranostics by replacing ^{62}Cu or ^{64}Cu with high-dose ^{64}Cu or ^{67}Cu in Cu-labeled radiopharmaceuticals.

References

1. Su LC, Ravanshad S, Owen Jr CA, McCall JT, Zollman PE, Hardy RM. A comparison of copper-loading disease in Bedlington terriers and Wilson's disease in humans. *Am J Phys.* 1982;243:G226–30.
2. Wadas TJ, Wong EH, Weisman GR, Anderson CJ. Copper chelation chemistry and its role in copper radiopharmaceuticals. *Curr Pharm Des.* 2007;13:3–16.
3. Hino-Shishikura A, Tateishi U, Shibata H, Yoneyama T, Nishii T, Torii I, Tateishi K, Ohtake M, Kawahara N, Inoue T. Tumor hypoxia and microscopic diffusion capacity in brain tumors: a comparison of (62)Cu-Diacetyl-Bis (N4-Methylthiosemicarbazone) PET/CT and diffusion-weighted MR imaging. *Eur J Nucl Med Mol Imaging.* 2014;41:1419–27.
4. Tamura K, Kurihara H, Yonemori K, Tsuda H, Suzuki J, Kono Y, Honda N, Kodaira M, Yamamoto H, Yunokawa M, Shimizu C, Hasegawa K, Kanayama Y, Nozaki S, Kinoshita T, Wada Y, Tazawa S, Takahashi K, Watanabe Y, Fujiwara Y. (64)Cu-DOTA-trastuzumab PET imaging in patients with HER2-positive breast cancer. *J Nucl Med.* 2013;54:1869–75.
5. Kurihara H, Hamada A, Yoshida M, Shimma S, Hashimoto J, Yonemori K, Tani H, Miyakita Y, Kanayama Y, Wada Y, Kodaira M, Yunokawa M, Yamamoto H, Shimizu C, Takahashi K, Watanabe Y, Fujiwara Y, Tamura K. (64)Cu-DOTA-trastuzumab PET imaging and HER2 specificity of brain metastases in HER2-positive breast cancer patients. *EJNMMI Res.* 2015;12(5):8.
6. Srivastava SC. Paving the way to personalized medicine: production of some promising therapeutic radionuclides at Brookhaven national laboratory. *Semin Nucl Med.* 2012;42:151–63.
7. Eht DA, Smith NA, Bowers DL et al. Copper-67 production on electron Linacs-Photonuclear technology development. In: Proceedings of the 14th international workshop on targetry and target chemistry, Vol. 1509 of AIP conference proceedings, pp. 157–61.
8. Szymański P, Frączek T, Markowicz M, Mikiciuk-Olasik E. Development of copper based drugs, radiopharmaceuticals and medical materials. *Biometals.* 2012;25:1089–112.
9. Williams HA, Robinson S, Julyan P, Zweit J, Hastings D. A comparison of PET imaging characteristics of various copper radioisotopes. *Eur J Nucl Med Mol Imaging.* 2005;32:1473–80.
10. McCarthy DW, Bass LA, Cutler PD, et al. High purity production and potential applications of copper-60 and copper-61. *Nucl Med Biol.* 1999;26:351–8.
11. Szelecsényi F, Kovács Z, Suzuki K, Okada K, Fukumura T, Mukai K. Formation of ⁶⁰Cu and ⁶¹Cu via Co + ³He reactions up to 70 MeV: production possibility of ⁶⁰Cu for PET studies. *Nucl Instrum Methods Phys Res B: Beam Interactions with Materials and Atoms.* 2004;222:364–70.
12. Szelecsényi F, Suzuki K, Kovács Z, Takei M, Okada K. Production possibility of ^{60,61}Cu radioisotopes by alpha induced reactions on cobalt for PET studies. *Nucl Instrum Methods Phys Res B: Beam Interactions with Materials and Atoms.* 2002;187:153–63.
13. Fukumura T, Okada K, Szelecsényi F, Kovács Z, Suzuki K. Practical production of ⁶¹Cu using natural Co target and its simple purification with a chelating resin for ⁶¹Cu-ATSM. *Radiochim Acta.* 2004;92:209–14.
14. Szelecsényi F, Kovács Z, Suzuki K, et al. Production possibility of ⁶¹Cu using proton induced nuclear reactions on zinc for PET studies. *J Radioanal Nucl Chem.* 2005;263:539–46.
15. Szelecsényi F, Steyn GF, Kovács Z, van der Walt TN, Suzuki K. Comments on the feasibility of ⁶¹Cu production by proton irradiation of Zn nat on a medical cyclotron. *Appl Radiat Isot.* 2006;64:789–91.
16. Rowshanfarzad P, Sabet M, Jalilian AR, Kamalidehghan M. An overview of copper radionuclides and production of ⁶¹Cu by proton irradiation of Zn nat at a medical cyclotron. *Appl Radiat Isot.* 2006;64:1563–73.
17. Das SS, Chattopadhyay S, Barua L, Das MK. Production of ⁶¹Cu using natural cobalt target and its separation using ascorbic acid and common anion exchange resin. *Appl Radiat Isot.* 2012;70:365–8.

18. Fukumura T, Okada K, Suzuki H, Nakao R, Mukai K, Szelecsényi F, Kovács Z, Suzuki K. An improved $^{62}\text{Zn}/^{62}\text{Cu}$ generator based on a cation exchanger and its fully remote-controlled preparation for clinical use. *Nucl Med Biol.* 2006;33:821–7.
19. Haynes NG, Lacy JL, Nayak N, Martin CS, Dai D, Mathias CJ, Green MA. Performance of a $^{62}\text{Zn}/^{62}\text{Cu}$ generator in clinical trials of PET perfusion agent ^{62}Cu -PTSM. *J Nucl Med.* 2000;41:309–14.
20. McCarthy DW, Shefer RE, Klinkowstein RE, et al. Efficient production of high-specific-activity ^{64}Cu using a biomedical cyclotron. *Nucl Med Biol.* 1997;24:35–43.
21. Alliot C, Michel N, Bonraisin A-C, et al. One step purification process for no-carrier-added ^{64}Cu produced using enriched nickel target. *Radiochim Acta.* 2011;99:627–30.
22. Obata A, Kasamatsu S, McCarthy DW, et al. Production of therapeutic quantities of ^{64}Cu using a 12 MeV cyclotron. *Nucl Med Biol.* 2003;30:535–9.
23. Zinn KR, Chaudhuri TR, Cheng T-P, Morris JS, Meyer Jr WA. Production of no-carrier-added ^{64}Cu from zinc metal irradiated under boron shielding. *Cancer.* 1994;73:774–8.
24. Vimalnath KV, Rajeswari A, Chirayil V, et al. Studies on preparation of ^{64}Cu using (n, γ) route of reactor production using medium flux research reactor in India. *J Radioanal Nucl Chem.* 2011;290:221–5.
25. Stoll T, Kastleiner S, Shubin YN, Coenen HH, Qaim SM. Excitation functions of proton induced reactions on ^{68}Zn from threshold up to 71 MeV, with specific reference to the production of ^{67}Cu . *Radiochim Acta.* 2002;90:309–13.
26. Medvedev DG, Mausner LF, Meinken GE, et al. Development of a large scale production of ^{67}Cu from ^{68}Zn at the high energy proton accelerator: closing the ^{68}Zn cycle. *Appl Radiat Isot.* 2012;70:423–9.
27. Green MA, Klippenstein DL, Tennison JR. Copper(II) Bis(thiosemicarbazone) complexes as potential tracers for evaluation of cerebral and myocardial blood flow with PET. *J Nucl Med.* 1988;29:1549–57.
28. Moi MK, Meares CF, McCall MJ, Cole WC, DeNardo SJ. Copper chelates as probes of biological systems: stable copper complexes with a macrocyclic bifunctional chelating agent. *Anal Biochem.* 1985;148(1):249–53.
29. Kukis D, Did H, Greiner DP, et al. A comparative study of copper-67 radiolabeling and kinetic stabilities of antibody-macrocyclic chelate conjugates. *Cancer.* 1994;73s:779–86.
30. Jones-Wilson TM, Deal KA, Anderson CJ, McCarthy DW, Kovacs Z, Motekaitis RJ, Sherry AD, Martell AE, Welch MJ. The in vivo behavior of copper-64-labeled azamacrocyclic complexes. *Nucl Med Biol.* 1998;25:523–30.
31. Green MA, Mathias CJ, Welch MJ, McGuire AH, Perry D, Fernandez-Rubio F, Perlmutter JS, Raichle ME, Bergmann SR. Copper-62-labeled pyruvaldehyde bis(N4-methylthiosemicarbazone)copper(II): synthesis and evaluation as a positron emission tomography tracer for cerebral and myocardial perfusion. *J Nucl Med.* 1990;31:1989–96.
32. Okazawa H, Yonekura Y, Fujibayashi Y, Mukai T, Nishizawa S, Magata Y, Ishizu K, Tamaki N, Konishi J. Measurement of regional cerebral blood flow with copper-62-PTSM and a three-compartment model. *J Nucl Med.* 1996;37:1089–93.
33. Krohn KA, Link JM, Mason RP. Molecular imaging of hypoxia. *J Nucl Med.* 2008;49:129S–48S.
34. Mees G, Dierckx R, Vangestel C, Van de Wiele C. Molecular imaging of hypoxia with radio-labelled agents. *Eur J Nucl Med Mol Imaging.* 2009;36:1674–86.
35. Mason RP, Zhao D, Pacheco-Torres J, Cui W, Kodibagkar VD, Gulaka PK, Hao G, Thorpe P, Hahn EW, Peschke P. Multimodality imaging of hypoxia in preclinical settings. *Q J Nucl Med Mol Imaging.* 2010;54:259–80.
36. Dearling JL, Lewis JS, Mullen GE, Welch MJ, Blower PJ. Copper bis(thiosemicarbazone) complexes as hypoxia imaging agents: structure-activity relationships. *J Biol Inorg Chem.* 2002;7:249–59.
37. Young H, Carnochan P, Zweit J, Babich J, Cherry S, Ott R. Evaluation of copper(II)-pyruvaldehyde bis (N-4-methylthiosemicarbazone) for tissue blood flow measurement using a trapped tracer model. *Eur J Nucl Med.* 1994;21:336–41.

38. Fujibayashi Y, Taniuchi H, Yonekura Y, Ohtani H, Konishi J, Yokoyama A. Copper-62-ATSM: a new hypoxia imaging agent with high membrane permeability and low redox potential. *J Nucl Med.* 1997;38:1155–60.
39. Dehdashti F, Mintun MA, Lewis JS, Bradley J, Govindan R, Laforest R, Welch MJ, Siegel BA. In vivo assessment of tumor hypoxia in lung cancer with 60Cu-ATSM. *Eur J Nucl Med Mol Imaging.* 2003;30:844–50.
40. Dehdashti F, Grigsby PW, Lewis JS, Laforest R, Siegel BA, Welch MJ. Assessing tumor hypoxia in cervical cancer by PET with 60Cu-labeled diacetyl-bis(N4-methylthiosemicarbazone). *J Nucl Med.* 2008;49:201–5.
41. Dietz DW, Dehdashti F, Grigsby PW, Malyapa RS, Myerson RJ, Picus J, Ritter J, Lewis JS, Welch MJ, Siegel BA. Tumor hypoxia detected by positron emission tomography with 60Cu-ATSM as a predictor of response and survival in patients undergoing Neoadjuvant chemoradiotherapy for rectal carcinoma: a pilot study. *Dis Colon Rectum.* 2008;51:1641–8.
42. Chao KS, Bosch WR, Mutic S, Lewis JS, Dehdashti F, Mintun MA, Dempsey JF, Perez CA, Purdy JA, Welch MJ. A novel approach to overcome hypoxic tumor resistance: Cu-ATSM-guided intensity-modulated radiation therapy. *Int J Radiat Oncol Biol Phys.* 2001;49:1171–82.
43. Lewis JS, Laforest R, Dehdashti F, Grigsby PW, Welch MJ, Siegel BA. An imaging comparison of 64Cu-ATSM and 60Cu-ATSM in cancer of the uterine cervix. *J Nucl Med.* 2008;49:1177–82.
44. Kinoshita T, Fujii H, Hayashi Y, Kamiyama I, Ohtsuka T, Asamura H. Prognostic significance of hypoxic PET using 18F-FAZA and 62Cu-ATSM in non-small-cell lung cancer. *Lung Cancer.* 2016;91:56–66.
45. Tateishi K, Tateishi U, Sato M, Yamanaka S, Kanno H, Murata H, Inoue T, Kawahara N. Application of 62Cu-Diacetyl-Bis (N4 -Methylthiosemicarbazone) PET imaging to predict highly malignant tumor grades and hypoxia-inducible factor-1 Expression in patients with Glioma. *AJNR.* 2013;34:92–9.
46. Buzdar AU, Ibrahim NK, Francis D, Boose DJ, Thomas ES, Theriault RL, et al. Significantly higher pathologic complete remission rate after neoadjuvant therapy with trastuzumab, paclitaxel, and epirubicin chemotherapy: results of a randomized trial in human epidermal growth factor receptor 2–positive operable breast cancer. *J Clin Oncol.* 2005;23:3676–85.
47. Piccart-Gebhart MJ, Procter M, Leyland-Jones B, Goldhirsch A, Untch M, Smith I, et al. Trastuzumab after adjuvant chemotherapy in HER2-positive breast cancer. *N Engl J Med.* 2005;353:1659–72.
48. Romond EH, Perez EA, Bryant J, Sumab VJ, Geyer Jr CE, Davidson NE, et al. Trastuzumab plus adjuvant chemotherapy for operable HER2-positive breast cancer. *N Engl J Med.* 2005;353:1673–84.
49. Slamon DJ, Leyland-Jones B, Shak S, Fuchs H, Paton V, Bajamonde A, et al. Use of chemotherapy plus a monoclonal antibody against HER2 for metastatic breast cancer that overexpresses HER2. *N Engl J Med.* 2001;344:783–92.
50. Tripathy D, Slamon DJ, Cobleigh M, Arnold A, Saleh M, Mortimer JE, et al. Safety of treatment of metastatic breast cancer with trastuzumab beyond disease progression. *J Clin Oncol.* 2004;22:1063–70.
51. Moasser MM. The oncogene HER2: its signaling and transforming functions and its role in human cancer pathogenesis. *Oncogene.* 2007;26:6469–87.
52. Hayes DF, Thor AD, Dressler LG, Weaver D, Edgerton S, Cowan D, et al. HER2 and response to paclitaxel in node-positive breast cancer. *N Engl J Med.* 2007;357:1496–506.
53. Sauter G, Lee J, Bartlett JM, Slamon DJ, Press MF. Guidelines for human epidermal growth factor receptor 2 testing: biologic and methodologic considerations. *J Clin Oncol.* 2009;27:1323–33.
54. Lebeau A, Turzynski A, Braun S, Behrhof W, Fleige B, Schmitt WD, et al. Reliability of human epidermal growth factor receptor 2 immunohistochemistry in breast core needle biopsies. *J Clin Oncol.* 2010;28:3264–70.

55. Xiao C, Gong Y, Han EY, Gonzalez-Angulo AM, Sneige N. Stability of HER2-positive status in breast carcinoma: a comparison between primary and paired metastatic tumors with regard to the possible impact of intervening trastuzumab treatment. *Ann Oncol.* 2011;22:1547–53.
56. Houssami N, Macaskill P, Balleine RL, Bilous M, Pegram MD. HER2 discordance between primary breast cancer and its paired metastasis: tumor biology or test artifact? Insights through metaanalysis. *Breast Cancer Res Treat.* 2011;129:659–74.
57. Dijkers EC, de Vries EG, Kosterink JG, Brouwers AH, Lub-de Hooge MN. Immunoscintigraphy as potential tool in the clinical evaluation of HER2/neu targeted therapy. *Curr Pharm Des.* 2008;14:3348–62.
58. Kurihara H, Hamada A, Yoshida M, Shimma S, Hashimoto J, Yonemori K, et al. ^{64}Cu -DOTA-trastuzumab PET imaging and HER2-specificity of brain metastases in HER2-positive breast cancer patients. *EJNMMI Res.* 2015, (in print).
59. Dijkers EC, Oude Munnink TH, Kosterink JG, Brouwers AH, Jager PL, de Jong JR, et al. Biodistribution of ^{89}Zr -trastuzumab and PET imaging of HER2-positive lesions in patients with metastatic breast cancer. *Clin Pharmacol Ther.* 2010;87:586–92.
60. Mortimer JE, Bading JR, Colcher DM, Conti PS, Frankel PH, Carroll MI, et al. Functional imaging of human epidermal growth factor receptor 2-positive metastatic breast cancer using ^{64}Cu -DOTA-trastuzumab PET. *J Nucl Med.* 2014;55:23–9.
61. Pfeifer A, Knigge U, Mortensen J, et al. Clinical PET of neuroendocrine tumors using ^{64}Cu -DOTATATE: First-in-Humans study. *J Nucl Med.* 2012;53:1207–15.